Heat Transfer Engineering, 29(9):793–804, 2008

ISSN: 0145-7632 print / 1521-0537 online
DOI: 10.1080/01457630802053827

Taylor & Francis
Taylor & Francis Group

Contribution Analysis of Dimensionless Variables for Laminar and Turbulent Flow Convection Heat Transfer in a Horizontal Tube Using Artificial Neural Network

LAP MOU TAM,[1] AFSHIN J. GHAJAR,[2] and HOU KUAN TAM[1]

[1]Department of Electromechanical Engineering, Faculty of Science and Technology, University of Macau, Taipa, Macau, China
[2]School of Mechanical and Aerospace Engineering, Oklahoma State University, Stillwater, Oklahoma, USA

The artificial neural network (ANN) method has shown its superior predictive power compared to the conventional approaches in many studies. However, it has always been treated as a "black box" because it provides little explanation on the relative influence of the independent variables in the prediction process. In this study, the ANN method was used to develop empirical correlations for laminar and turbulent heat transfer in a horizontal tube under the uniform wall heat flux boundary condition and three inlet configurations (re-entrant, square-edged, and bell-mouth). The contribution analysis for the dimensionless variables was conducted using the index of contribution defined in this study. The relative importance of the independent variables appearing in the correlations was examined using the index of contribution based on the coefficient matrices of the ANN correlations. For the turbulent heat transfer data, the Reynolds and Prandtl numbers were observed as the most important parameters, and the length-to-diameter and bulk-to-wall viscosity ratios were found to be the least important parameters. The method was extended to analyze the more complicated forced and mixed convection data in developing laminar flow. The dimensionless parameters influencing the heat transfer in this region were the Rayleigh number and the Graetz number. The contribution analysis clearly showed that the Rayleigh number has a significant influence on the mixed convection heat transfer data, and the forced convection heat transfer data is more influenced by the Graetz number. The results of this study clearly indicated that the contribution analysis method can be used to provide correct physical insight into the influence of different variables or a combination of them on complicated heat transfer problems.

INTRODUCTION

Heat transfer inside horizontal tubes in the laminar, transitional, and turbulent flow regimes have been studied experimentally by various researchers in the past. Usually, the experimental results are presented in the form of heat transfer correlations. The form of the correlations is based either on different theoretical models or are completely empirical-based. The coefficients of the correlations are usually determined by the conventional least squares method. Kakac et al. [1] and Tam and Ghajar [2] documented some of the most well-accepted correlations in the above-mentioned flow regimes.

Ghajar et al. [3] used an unconventional method, the artificial neural network (ANN), to very successfully correlate the transitional heat transfer experimental data of Ghajar and Tam [4] for three different inlet configurations. Their ANN heat transfer correlation when compared with the conventional least squares based correlation of Ghajar and Tam [4] showed to be more accurate [3]. However, as briefly discussed in Ghajar et al. [3], although the ANN method is superior in its predictive power in comparison to the conventional methods, it provides little explanation as to the relative importance of the independent variables that appear in these correlations.

Address correspondence to Dr. Afshin J. Ghajar, School of Mechanical and Aerospace Engineering, Oklahoma State University, Stillwater, Oklahoma 74078, USA. E-mail: afshin.ghajar@okstate.edu

The objective of this study was to develop the necessary methods to identify the least and most important variables that appear in the heat transfer correlations developed based on the ANN method. For this purpose, the ANN method was used to correlate the experimental data of Ghajar and Tam [4] for laminar and turbulent heat transfer in a horizontal tube under the uniform wall heat flux boundary condition and three inlet configurations (re-entrant, square-edged and bell-mouth). It should be noted that the transition region heat transfer data of Ghajar and Tam [4] was not considered is this study because, due to the complicated nature of the transition region, every dimensionless parameter in their [3] ANN transition heat transfer correlation is important. Thus, the use of the transition data would not be beneficial in clearly demonstrating the capability of the method proposed in this study.

HEAT TRANSFER EXPERIMENTS

The heat transfer experimental data used in this study, along with a detailed description of the experimental apparatus and procedures used, were reported in Ghajar and Tam [4]. A schematic of the overall experimental setup used for heat transfer measurements is shown in Figure 1. In this paper, only a brief description of the experimental setup and procedures will be provided. The local forced and mixed convective measurements were made in a horizontal, electrically heated, stainless steel circular straight tube under uniform wall heat flux boundary condition and three types of inlet configurations (re-entrant, square-edged, and bell-mouth), as shown in Figure 2. The pipe had an inside diameter of 1.58 cm and an outside diameter of 1.90 cm. The total length of the test section was 6.10 m, providing a maximum length-to-inside diameter ratio of 385. A uniform wall heat flux boundary condition was maintained by a DC arc welder. Thermocouples (T-type) were placed on the outer surface of the tube wall at close intervals near the entrance and at greater intervals further downstream. Twenty-six axial locations were designated, with four thermocouples placed at each location. The thermocouples were placed 90° apart around

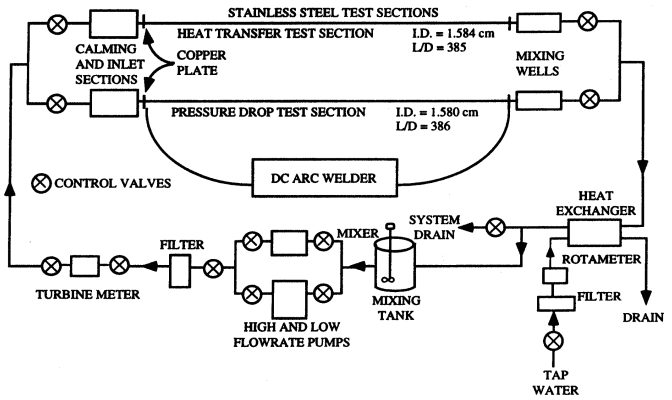

Figure 1 Schematic diagram of experimental setup.

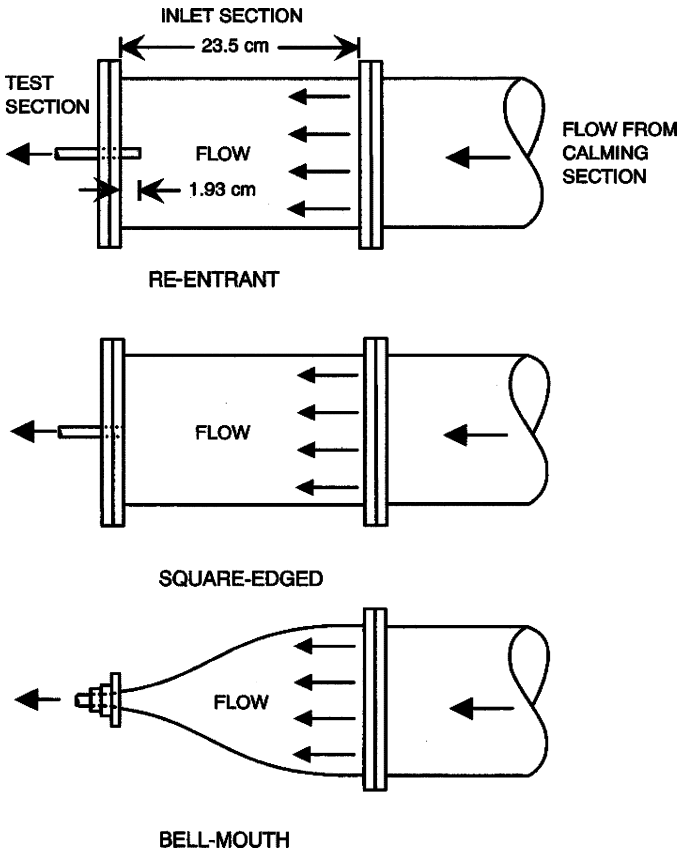

Figure 2 Schematic of the three different inlet configurations.

the periphery. From the local peripheral wall temperature measurements at each axial location, the inside wall temperatures and the local heat transfer coefficients were calculated [5]. In these calculations, the axial conduction was assumed negligible (RePr > 4,200 in all cases), but peripheral and radial conduction of heat in the tube wall were included. In addition, the bulk fluid temperature was assumed to increase linearly from the inlet to the outlet. As reported by Ghajar and Tam [4], the uncertainty analyses of the overall experimental procedures showed that there is a maximum of 9% uncertainty for the heat transfer coefficient calculations. Moreover, the heat balance error for each experimental run indicates that in general, the heat balance error is less than 5%. For Reynolds numbers lower than 2,500, where the flow is strongly influenced by secondary flow, the heat balance error is slightly higher (5–8%) for that particular Reynolds number range.

To ensure a uniform velocity distribution in the test fluid before it entered the test section, the flow passed through calming and inlet sections. The calming section had a total length of 61.6 cm and consisted of a 17.8 cm-diameter acrylic cylinder with three perforated acrylic plates, followed by tightly packed soda straws sandwiched between galvanized steel mesh screens. Before entering the inlet section, the test fluid passed through a fine mesh screen and flowed undisturbed through 23.5 cm of a 6.5 cm-diameter acrylic tube before it entered the test

section. The inlet section had the versatility of being modified to incorporate a re-entrant or bell-mouth inlet (see Figure 2). The re-entrant inlet was simulated by sliding 1.93 cm of the tube entrance length into the inlet section, which was otherwise the square-edged (sudden contraction) inlet. For the bell-mouth inlet, a fiberglass nozzle with contraction ratio of 10.7 and a total length of 23.5 cm was used in place of the inlet section.

In their experiments, Ghajar and Tam [4] used distilled water and mixtures of distilled water and ethylene glycol. They collected 1,150 experimental data points for the laminar and turbulent regions, and their experiments covered a local bulk Reynolds number range of 280 to 49,000, a local Prandtl number range of 4 to 158, a local bulk Grashof number range of 1,000 to 2.5×10^5, and a local bulk Nusselt number range of 13 to 258. The wall heat flux for their experiments ranged from 4 to 670 kW/m^2.

HEAT TRANSFER CHARACTERISTICS IN THE LAMINAR AND TURBULENT REGIONS

Before analyzing the heat transfer data, it is important to review the heat transfer characteristics of the flow in the laminar and turbulent regions.

The application of heat to the tube wall produces a temperature difference in the fluid. The fluid near the tube wall has a higher temperature and lower density than the fluid close to the centerline of the tube. This temperature difference may produce a secondary (vortex-like) flow due to free convection. The boundary between the mixed and forced convection, according to Ghajar and Tam [6], can be determined from the local peripheral heat transfer coefficient at the top of the tube to the local peripheral heat transfer coefficient at the bottom of the tube (h_t/h_b). The ratio should be close to unity (0.8–1.0) for forced convection and is much less than unity (<0.8) for a case in which mixed convection exists. To illustrate the different heat transfer modes (mixed and forced convection) encountered for the three inlets used in the experiments of [4], Figure 3 is presented. This figure shows the effect of secondary flow on heat transfer coefficient ratio h_t/h_b, for different inlets, flow regimes, and the length-to-diameter ratio (distance from the inlet). It includes representative Reynolds number ranges from laminar to fully turbulent flow (Re = 280–49,000) for the three inlets. As shown in the figure, the boundary between the forced and mixed convection heat transfer is inlet-dependent. For the re-entrant, square-edged, and bell-mouth inlets, when the Reynolds numbers were greater than 2,500, 3,000, and 8,000, respectively, the flows were dominated by forced convection heat transfer, and the heat transfer coefficient ratios (h_t/h_b) did not fall below 0.8–0.9. In fact, at times they exceeded unity due to the roundoff errors in the property evaluation subroutine of their [5] data reduction program.

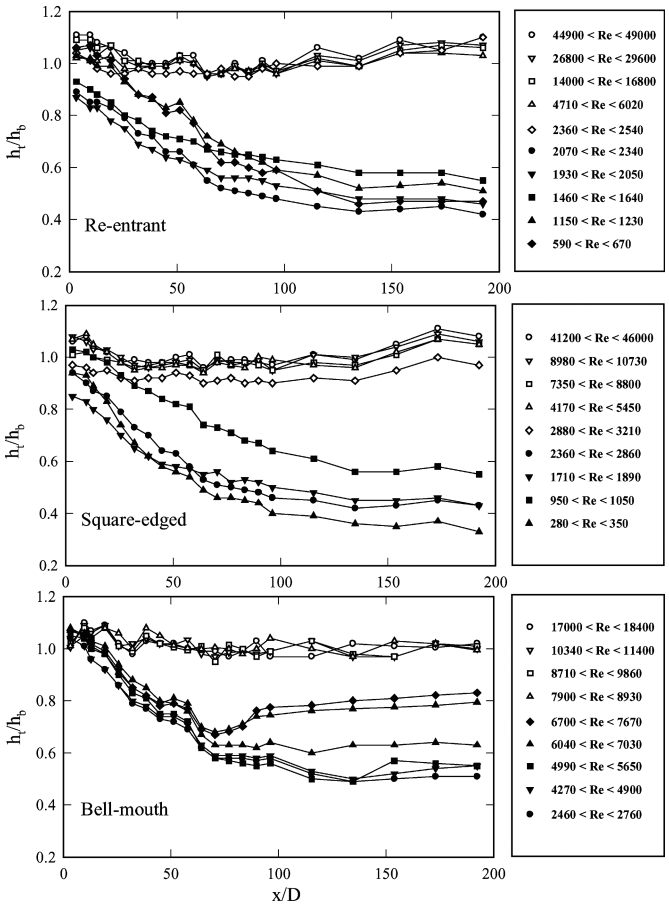

Figure 3 Effect of secondary flow on heat transfer coefficient for different inlets and flow regimes.

However, the free convection effect was observed to be more significant for the low Reynolds number flows. For the low Reynolds number flows dominated by mixed convection heat transfer, the h_t/h_b ratio began near 1 at the tube entrance, indicating that the flow was initially dominated by the forced convection, but dropped off rapidly as the length-to-diameter ratio (x/D) increased. Beyond about 125 diameters from the tube entrance, the ratio was almost invariant with x/D, indicating a much less dominant role for forced convection heat transfer and an increased free convection activity.

Based on the above observations, mixed convection only appeared in the laminar heat transfer data. Therefore, it can be concluded that the laminar Nusselt number (dimensionless heat transfer coefficient) is a function of five dimensionless variables, Re, Pr, Gr, x/D, and μ_b/μ_w. The ranges of dimensionless variables considered in this study for laminar flow are:

$13 \le \text{Nu} \le 65$; $280 \le \text{Re} \le 3800$
$40 \le \text{Pr} \le 160$; $1000 \le \text{Gr} \le 2.8 \times 10^4$
$3 \le \text{x/D} \le 192$; $1.2 \le \mu_b/\mu_w \le 3.8$

Table 1 Prediction results for the laminar flow correlation developed based on the least squares method, Eq. (1)

Inlet configuration	Number of data within ±10%	Number of data within ±5%	Abs. mean dev. (%)	Abs. range of dev. (%)
Forced convection				
Total data points for all three inlets (212 pts.)	183	113	5.4	−15.4% to +16.9%
Re-entrant (84 pts.)	71	41	5.9	−9.5% to +16.9%
Square-edged (96 pts.)	80	62	4.7	−15.4% to +13.4%
Bell-mouth (32 pts.)	32	10	6.1	+2.7% to +9.8%
Mixed convection				
Total data points for all three inlets (334 pts.)	282	148	6.0	−13.7% to +16.5%
Re-entrant (84 pts.)	83	51	4.1	−9.5% to +13.3%
Square-edged (198 pts.)	163	80	6.4	−13.7% to +16.5%
Bell-mouth (52 pts.)	36	17	7.7	+1.9% to +15.1%

Ghajar and Tam [4] collected a total of 546 experimental data points for the three inlets: 168 for the re-entrant, 294 for the square-edged, and 84 for the bell-mouth. The experimental data for the laminar forced and mixed convection in the entrance and fully developed flow regions for all three inlets were then correlated in a form similar to the one proposed by Martinelli and Boelter [7].

$$\mathrm{Nu_l} = 1.24[(\mathrm{RePrD/x}) + 0.025(\mathrm{GrPr})^{0.75}]^{1/3}(\mu_b/\mu_w)^{0.14} \quad (1)$$

The accuracy of the correlation is described in Table 1. The total number of data points for forced convection (212 data points) is predicted within −15.4% to +16.9%, and those for mixed convection (334 data points) are predicted within −13.17% to +16.5%. Greater than 85% of all the data are predicted within ±10% deviation for the two convection modes. For forced convection, about 53% of all the data (113 data points) are predicted within ±5% deviation, and the absolute mean deviation is 5.4%. For the mixed convection, about 53% of all the data (148 data points) are predicted within ±5% deviation, and the absolute mean deviation is 6.0%.

Regarding the turbulent region, the turbulent Nusselt number is a function of the dimensionless variables, Re, Pr, x/D, and μ_b/μ_w. Unlike the laminar region, Gr is not considered here because the buoyancy effect is not important in the turbulent region. The ranges of the dimensionless variables considered in this study for turbulent flow are summarized as follows:

$52.3 \le \mathrm{Nu} \le 242.4$; $7{,}000 \le \mathrm{Re} \le 49{,}000$
$4.0 \le \mathrm{Pr} \le 34.0$; $3.2 \le \mathrm{x/D} \le 173.1$
$1.1 \le \mu_b/\mu_w \le 1.7$

Similar to the correlation form proposed by Sieder and Tate [8], Ghajar and Tam [4] developed the following correlation for their turbulent forced convection data in the entrance and fully developed regions for all three inlets:

$$\mathrm{Nu_t} = 0.023\mathrm{Re}^{0.8}\mathrm{Pr}^{0.385}(\mathrm{x/D})^{-0.0054}(\mu_b/\mu_w)^{0.14} \quad (2)$$

Table 2 Prediction results for the turbulent flow correlation developed based on the least squares method, Eq. (2)

Inlet configuration	Number of data within ±10%	Number of data within ±5%	Abs. mean dev. (%)	Abs. range of dev. (%)
Total data points for all three inlets (604 pts.)	600	439	4.4	−10.3% to +10.6%
Re-entrant (271 pts.)	269	192	3.9	−9.2% to +10.6%
Square-edged (207 pts.)	206	153	3.6	−8.7% to +10.1%
Bell-mouth (126 pts.)	125	94	3.5	−10.3% to +4.1%

A total of 604 data points were used to develop the above correlation, correlating 100% of experimental data with less than ±11% deviation and 73% of the measured data with less than ±5% deviation. The details are given in Table 2.

GENERAL DEFINITION OF ANN CORRELATION AND THE INDEX OF CONTRIBUTION ANALYSIS

To correlate the data in general, the ANN with single hidden layer is employed. Figure 4 shows a typical example of ANN model of this kind. It has been shown that any continuous correlation can be modeled by the network [9]. The weight and the bias of the optimal ANN model are usually determined by the back propagation algorithms [10]. In order to determine the contribution of each independent variable to the correlation, the matrix form of the optimal ANN model as shown by Eq. (3) has to be examined first.

$$\mathrm{N}(\mathrm{p_1}, \cdots, \mathrm{p_R}) = \left[\mathrm{w_1^2}, \cdots, \mathrm{w_S^2}\right] \begin{bmatrix} f\left(\sum_{j=1}^{R} w_{1j}^1 p_j + b_1^1\right) \\ f\left(\sum_{j=1}^{R} w_{2j}^1 p_j + b_2^1\right) \\ \vdots \\ f\left(\sum_{j=1}^{R} w_{Sj}^1 p_j + b_S^1\right) \end{bmatrix} + \mathrm{b_1^2} \quad (3)$$

where $(\mathrm{p_1}, \cdots, \mathrm{p_R})$ are the R inputs, S is the number of hidden neurons, $\mathrm{f(t)} = \frac{1}{1+\mathrm{e}^{-\mathrm{t}}}$ is the transfer function, and w's and b's

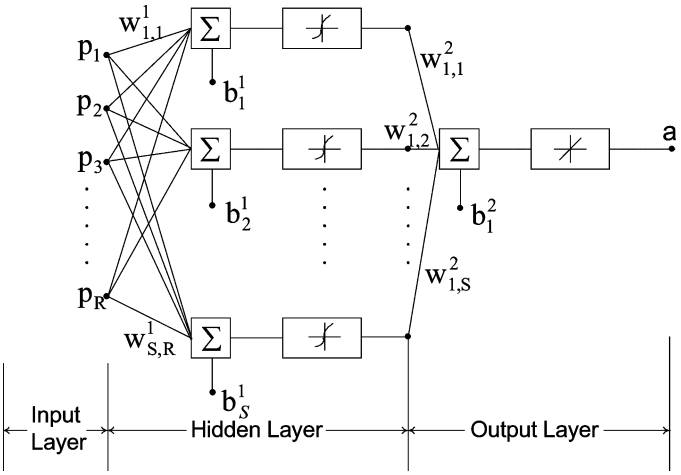

Figure 4 A three-layer ANN with S neurons in its hidden layer.

are the weights and biases of the ANN, respectively. The contribution of the independent variables p_j to the output of the kth neuron in the hidden layer $f(\sum_{j=1}^{R} w_{kj}^1 p_j + b_k^1)$ is simply $|w_{kj}^1|$ and the relative contribution of the kth neuron output to the ANN model is defined as:

$$Q_k = \frac{|w_k^2|}{\sum_{i=1}^{S} |w_i^2|} \tag{4}$$

Therefore, the contribution of the independent variables p_j to the ANN model is:

$$P_j = \sum_{k=1}^{S} Q_k * \left|w_{kj}^1\right| \tag{5}$$

Finally, in order to compare with the other independent variables, the index of contribution of p_j is defined to be

$$\text{index}(p_j) = \frac{P_j}{\sum_{i=1}^{R} P_i} \times 100\% \tag{6}$$

Hence, the most significant independent variable would have the largest index of contribution. On the other hand, the variable with small index appears to be less important.

ANALYSIS OF THE TURBULENT AND LAMINAR DATA USING THE INDEX OF CONTRIBUTION

For the turbulent data, before using the index of contribution defined in Eq. (6), it is worthwhile to evaluate the traditional least squares correlation given by Eq. (2). According to the form of Eq. (2), it is obvious that Reynolds and Prandtl numbers are both important. However, it is not possible to tell which one is more important than the other by simply judging the exponents of them. It is also obvious that x/D and μ_b/μ_w are the least important variables. According to the ranges of the data used in the development of Eq. (2), the value of the terms $(x/D)^{-0.0054}$ and $(\mu_b/\mu_w)^{0.14}$ are very close to unity, hence they made less contribution to the Nusselt number. Theoretically, for turbulent flow, the thermal entry length is usually very short and the entrance effect is insignificant. Moreover, from Sieder and Tate [8], the data in the turbulent region show little variation between μ_b and μ_w because, first, fluids that give turbulent flow seldom have a large kinematic viscosity, and, second, because the heat transfer rates are high, preventing large temperature differences. Therefore, both the terms $(x/D)^{-0.0054}$ and $(\mu_b/\mu_w)^{0.14}$ act as correction factors to make the correlation more accurate.

Coming back to the ANN analysis, using the supervised three-layer feedforward neural network with fully weighted connection and the algorithm described in the previous section to determine the index of contribution for each independent variable, we need to decide on (a) the gradient method to be used, and (b) the reasonable number of iterations and neurons to be used for each network training.

For the gradient method to be used, according to Ghajar et al. [3], the Levenberg-Marquardt algorithm (LM) was adopted as the gradient method in back-propagation. According to Hagan and Menhaj [11], this method can speed up the network training. However, it is hard to tell whether this method works well with the index of contribution analysis. Therefore, in this study, the classical gradient method, which is the slower steepest descent algorithm (SDA), is also considered. The turbulent heat transfer data is correlated using both the LM and SDA methods. The number of neurons was varied from 5 to 8, and the iteration for each training was fixed at 10,000. The index of contribution based on the algorithm described in the previous section using different number of neurons was calculated and is shown in Figure 5. Each data point shown in the figure is an average of 10 trainings. From Figure 5, it is obvious that the SDA method (see Figure 5a) gave more consistent information regarding the

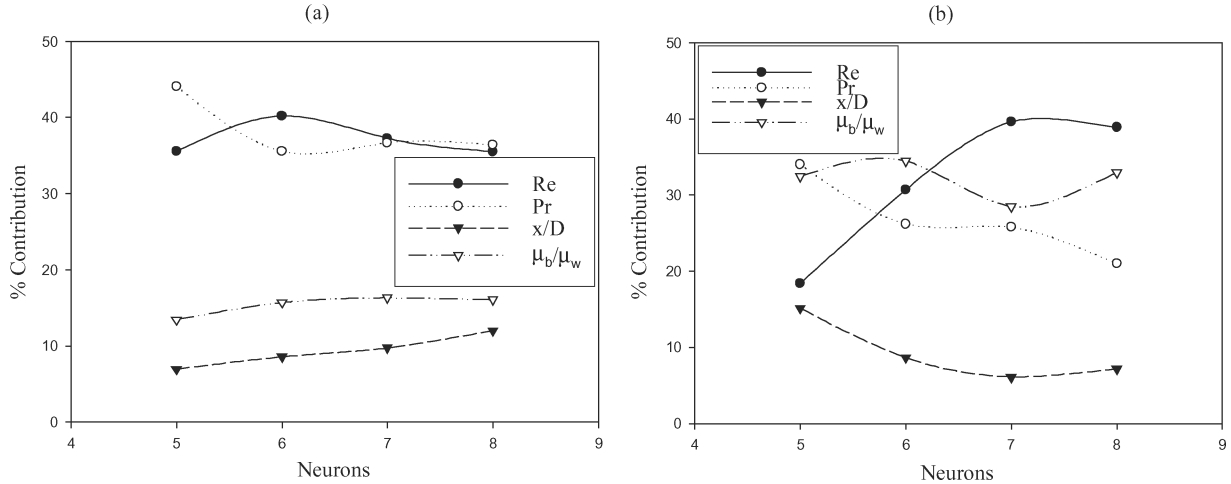

Figure 5 A comparison of the percent contribution by using two different gradient descent algorithms: (a) Slower algorithm = SDA method; (b) Faster algorithm = LM method. Each data point shown is the average value from 10 trainings.

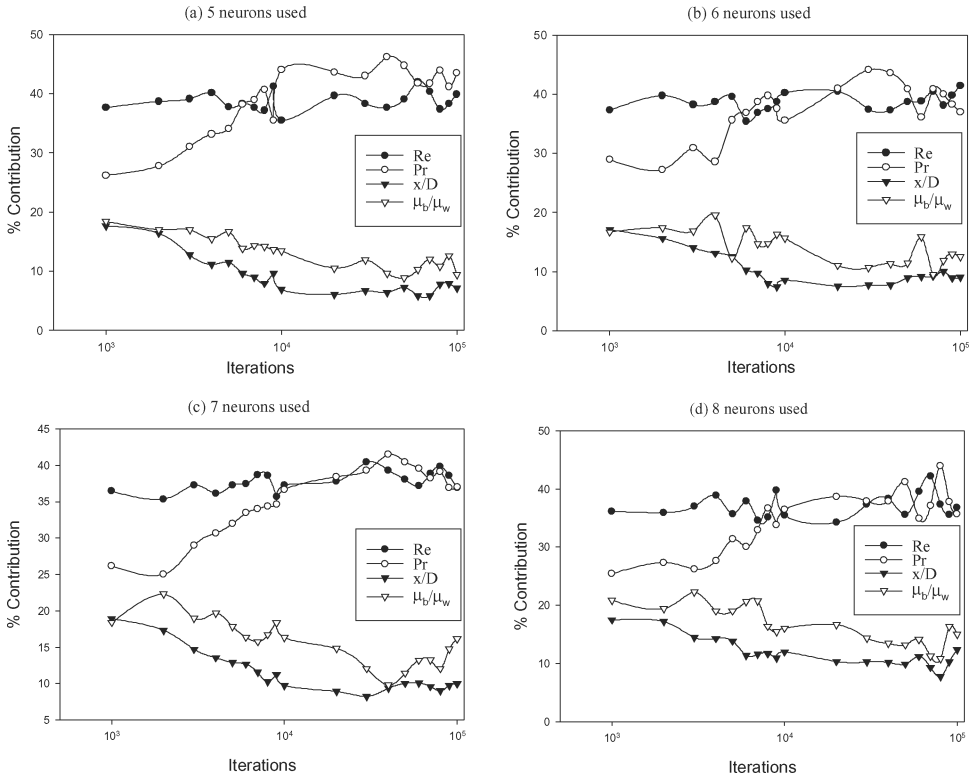

Figure 6 The percent contribution from ANN training for different dimensionless numbers to Nusselt number by adjusting the iterations and the number of neurons: (a) five neurons, (b) six neurons, (c) seven neurons, and (d) eight neurons. Each data point is the average value from 10 trainings.

contribution from each independent variable regardless of how many neurons were used. Moreover, the findings based on SDA agree with the findings according to the traditional least squares equation, where Re and Pr contribute the most, and $(x/D)^{-0.0054}$ and $(\mu_b/\mu_w)^{0.14}$ contribute the least. When the LM method is considered (see Figure 5b), the influence of $(\mu_b/\mu_w)^{0.14}$ is large, and the same observations cannot be seen. Because $(\mu_b/\mu_w)^{0.14}$ is proved to be a correction factor in the turbulent region, the LM method cannot clearly identify the contribution of each variable. Therefore, the SDA method should be selected as the gradient method for this study.

Regarding the number of hidden neurons and training iterations employed, it was determined by the observations of the computations based on their different combinations. According to Eq. (3), the Re, Pr, x/D, and μ_b/μ_w were treated as the input variables and the Nu was used as the output variable for the training of ANN. As depicted in Figure 6, it is apparent that the index of contribution is consistent at the beginning of the 10,000 iterations regardless of the number of neurons. The index of Re and Pr were close to 40% but both ratios (x/D, μ_b/μ_w) contributed less than 20%.

Based on the observations made above, the gradient method chosen was SDA, the number of iterations used was 10,000, the number of neurons used was taken as 6, and the form of the ANN correlation used is given by Eq. (3). With the establishment of the ANN correlation, the index of contribution according to the above mentioned criteria can now be computed. For reliability purposes, ninety percent of the 604 data points were used for training, and the remaining data were involved for verification. The initial value of the free parameters (weights and biases) was randomly selected within ± 1. For satisfying the log-sigmoid transfer function, the normalized input variables, Reynolds number, Prandtl number, length-to-diameter ratio, and viscosity ratio are arranged into the input vector, p, as shown below:

$$\mathrm{p} = \begin{bmatrix} \mathrm{Re}_{\mathrm{normal}} \\ \mathrm{Pr}_{\mathrm{normal}} \\ \left(\dfrac{x}{D}\right)_{\mathrm{normal}} \\ \left(\dfrac{\mu_b}{\mu_w}\right)_{\mathrm{normal}} \end{bmatrix} = \begin{bmatrix} 2\cdot[\mathrm{Re}-\mathrm{Re}_{\min}]/[\mathrm{Re}_{\max}-\mathrm{Re}_{\min}]-1 \\ 2\cdot[\mathrm{Pr}-\mathrm{Pr}_{\min}]/[\mathrm{Pr}_{\max}-\mathrm{Pr}_{\min}]-1 \\ 2\cdot\left[\left(\dfrac{\mathrm{x}}{\mathrm{D}}\right)-\left(\dfrac{\mathrm{x}}{\mathrm{D}}\right)_{\min}\right]\Big/\left[\left(\dfrac{\mathrm{x}}{\mathrm{D}}\right)_{\max}-\left(\dfrac{\mathrm{x}}{\mathrm{D}}\right)_{\min}\right]-1 \\ 2\cdot\left[\left(\dfrac{\mu_b}{\mu_w}\right)-\left(\dfrac{\mu_b}{\mu_w}\right)_{\min}\right]\Big/\left[\left(\dfrac{\mu_b}{\mu_w}\right)_{\max}-\left(\dfrac{\mu_b}{\mu_w}\right)_{\min}\right]-1 \end{bmatrix} \tag{7}$$

Table 3 Prediction results for the improved turbulent flow correlation developed based on the ANN method

Inlet configuration	Number of data within ±10%	Number of data within ±5%	Abs. mean dev. (%)	Abs. range of dev. (%)
Total data points for all three inlets (604 pts.)	598	456	3.4	−16.8% to +9.8%
Re-entrant (271 pts.)	268	187	3.9	−10.9% to +9.8%
Square-edged (207 pts.)	204	169	2.9	−16.8% to +9.2%
Bell-mouth (126 pts.)	126	100	3.2	−7.9% to +9.1%

See Eqs. (3) and (7) for the input vector (p) and Eq. (8) for the constant matrices and scalars (w^1, w^2, b^1, b^2)

In Eq. (3), the dependent output is the Nusselt number for the turbulent heat transfer data. The w^1, w^2, b^1, b^2 terms used in Eq. (3) are constant matrices and scalars. Their numerical values are shown in the following matrices:

$$w^1 = \begin{bmatrix} 0.69 & -0.19 & 0.56 & 0.79 \\ 1.09 & 0.08 & 0.62 & 0.64 \\ 1.56 & -0.60 & -0.01 & -0.48 \\ -0.93 & -2.21 & 0.10 & -0.08 \\ -0.32 & 0.86 & 0.57 & 0.89 \\ -0.11 & 0.96 & -0.79 & -0.05 \end{bmatrix},$$

$$w^2 = \begin{bmatrix} 0.53 & 0.41 & 1.81 & -2.43 & -0.85 & -0.12 \end{bmatrix},$$

$$b^1 = \begin{bmatrix} 0.73 \\ -0.31 \\ 1.24 \\ -1.73 \\ -0.62 \\ 0.16 \end{bmatrix}, b^2 = -0.36 \quad (8)$$

As shown in Table 3, all the experimental data were predicted within −16.8% to +9.8%. The absolute deviation of all the predictions is around 3.4%. About 99% of all the data (598 data points) were predicted within ±10% deviation. About 75% of all the data (456 data points) were predicted within ±5% deviation. As compared to the results of the turbulent heat transfer correlation given by Eq. (2) and presented in Table 2, the good accuracy in predicting the turbulent experimental data was maintained by the ANN correlation.

For the calculation of the index of contribution for each variable, Eqs. (4–6) were employed according to the weight matrices, w^1 and w^2, given in Eq. (8). The computation process is completed in three steps as shown below:

1. For each hidden neuron k, the absolute value of the hidden-output layer connection weight is divided by the summation of the hidden-output layer connection weight, as seen in Eq. (4).

Step 1	Hidden neuron 1	Hidden neuron 2	Hidden neuron 3	Hidden neuron 4	Hidden neuron 5	Hidden neuron 6
Q_k	0.087	0.067	0.295	0.395	0.137	0.019

2. For each hidden neuron k, multiply the Q_k by the absolute value of the hidden-input layer connection weight. Then, sum up the values to obtain the P_j for each input variable p_j, as seen in Eq. (5).

Step 2	Re	Pr	x/D	μ_b/μ_w
P_j	1.008	1.207	0.227	0.407

3. Compute the index of contribution in percentage by dividing P_j by the sum of the P_j corresponding to each input variable, as seen in Eq. (6). The index of contribution for each variable is established as:

Step 3	Re	Pr	x/D	μ_b/μ_w
index (p_j)	35.4%	42.4%	7.9%	14.3%

The contribution analysis applied to the turbulent heat transfer and presented above will next be applied to the laminar heat transfer data. The laminar heat transfer data is more complicated because the entrance effect, buoyancy, and variation of properties are all important. Based on Figure 3, it can be observed that, regardless of which inlet configuration is used, secondary flow requires a certain length to develop. Therefore, we can conclude that the developing flow near the entrance is dominated by forced convection. When the flow is further downstream, mixed convection is the dominant mode of convection. Because of that, it would be reasonable to consider the first dimensionless group (RePrD/x) in Eq. (1), which is the so-called Graetz number (Gz), to take care of the forced convection heat transfer in the thermally developing region. The second dimensionless group (GrPr) in Eq. (1), which is referred to as the Rayleigh number (Ra), takes into consideration the effect of free convection. Careful observation of Eq. (1) reveals that the formation of the equation is in fact the superposition of a forced and a free convective heat transfer correlation. The last dimensionless group (μ_b/μ_w) in Eq. (1) accounts for the variation of physical properties due to heating. Because the wall-to-bulk temperature difference is much higher in the laminar region, this term is also important. Therefore, Eq. (1) can be represented

as:

$$Nu_l = 1.24[(Gz) + 0.025(Ra)^{0.75}]^{1/3}(\mu_b/\mu_w)^{0.14} \quad (9)$$

The advantages of the above arrangement are that the physical meanings of the dimensionless parameters are clearer, and the contribution analysis procedures can be simplified because the number of dimensionless variables to be considered have been reduced from 5 to 3. Therefore, our contribution analysis regarding the contributions from different dimensionless numbers in convective heat transfer in laminar flow is based on Gz, Ra, and μ_b/μ_w. As shown in Figure 3, at small length-to-diameter ratios (near the tube entrance), the free convection is still not established, and the flow is dominated by the forced convection based on the heat transfer coefficient ratios ($h_t/h_b > 0.8$). Therefore, the Rayleigh number is not an important parameter for the heat transfer in that region. However, as the length-to-diameter ratio is increased (20–70 diameters passed the tube entrance depending on the inlet configuration), the heat transfer mode is dominated by mixed convection, and the Rayleigh number becomes an important parameter.

For the analysis of the laminar flow heat transfer data, the 546 data points for the three different inlet configurations were divided into two sets of forced convection data with $h_t/h_b > 0.8$ and mixed convection data with $h_t/h_b < 0.8$. Out of the 546 data points, 212 data points were categorized as forced convection and the remaining data points were considered to be mixed convection. In the ANN training, the gradient method, number of hidden neurons employed, and the number of iterations used had to be determined. In accordance with the analysis for the turbulent heat transfer data, the steepest descent gradient algorithm (SDA) gave consistent results, so it was also used for the laminar heat transfer data. For the determination of the number of iterations and hidden neurons, the data sets were trained with four to seven neurons. The number of iterations for each training ranged from 1,000 to 100,000 times. The increment of iterations was set as 2,000 when the number of iterations was from 1,000 to 10,000. However, when the number of iterations was from 10,000 to 100,000, the increment of iterations was increased to 10,000. As shown in Figure 7, the trend of the contribution of each variable is consistent regardless of how many hidden neurons were employed. After 50,000

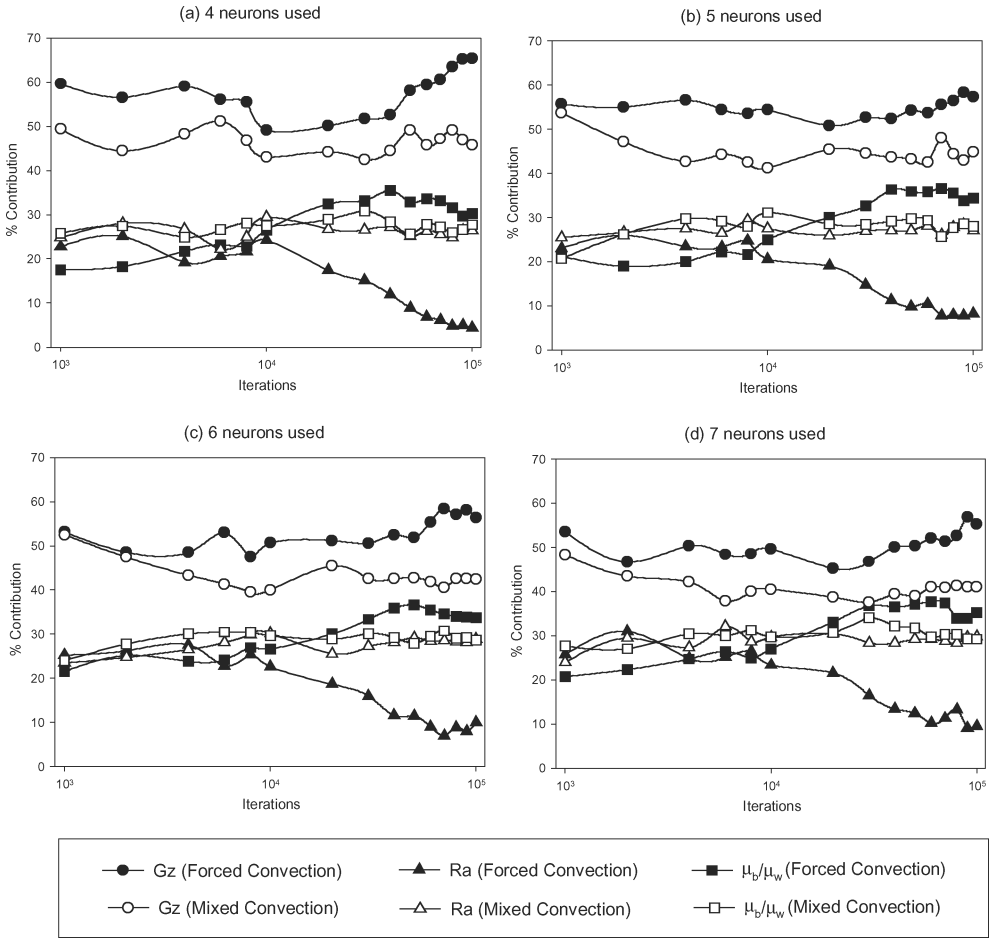

Figure 7 The percent contribution from ANN training for different dimensionless numbers to Nusselt number by adjusting the iterations and the number of neurons for forced and mixed convection: (a) four neurons, (b) five neurons, (c) six neurons, and (d) seven neurons. Each data point is the average value from 10 trainings.

iterations, the contribution curves of each variable were very well established.

Based on the observations made above, the number of iterations to be used was chosen as 50,000, the number of neurons to be used was arbitrarily selected as six, and the form of the ANN correlation to be used is given by Eq. (3). With the establishment of the ANN correlation, the index of contribution according to the above-mentioned criteria can then be computed. For reliability purposes, ninety percent of the total data points were used for training, and the remaining data was used for verification. The initial value of the free parameters (weights and biases) was randomly selected within ± 1. For satisfying the log-sigmoid transfer function, the normalized input variables, Graetz number, Rayleigh number, and viscosity ratio are arranged into the input vector, p, as shown below:

$$\mathrm{p} = \begin{bmatrix} \mathrm{Gz}_{\mathrm{normal}} \\ \mathrm{Ra}_{\mathrm{normal}} \\ \left(\frac{\mu_b}{\mu_w}\right)_{\mathrm{normal}} \end{bmatrix} \tag{10}$$

$$= \begin{bmatrix} 2 \cdot [\mathrm{Gz} - \mathrm{Gz}_{\min}]/[\mathrm{Gz}_{\max} - \mathrm{Gz}_{\min}] - 1 \\ 2 \cdot [\mathrm{Ra} - \mathrm{Ra}_{\min}]/[\mathrm{Ra}_{\max} - \mathrm{Ra}_{\min}] - 1 \\ 2 \cdot \left[\left(\frac{\mu_b}{\mu_w}\right) - \left(\frac{\mu_b}{\mu_w}\right)_{\min}\right] \Big/ \left[\left(\frac{\mu_b}{\mu_w}\right)_{\max} - \left(\frac{\mu_b}{\mu_w}\right)_{\min}\right] - 1 \end{bmatrix}$$

In Eq. (3), the dependent output is the Nusselt number for the laminar heat transfer data. The w^1, w^2, b^1, b^2 terms used in Eq. (3) are constant matrices and scalars. Their numerical values for forced and mixed convection heat transfer are shown separately in the following matrices.

For forced convection:

$$w^1 = \begin{bmatrix} -3.20 & 0.12 & 1.09 \\ 1.06 & 0.31 & 1.45 \\ 0.17 & 0.49 & 2.24 \\ -0.55 & 0.58 & 0.12 \\ -0.66 & 0.11 & -0.47 \\ 0.56 & 0.71 & -0.28 \end{bmatrix},$$

$$w^2 = \begin{bmatrix} -3.18 & 1.14 & 1.37 & -1.05 & -0.47 & 0.09 \end{bmatrix},$$

$$b^1 = \begin{bmatrix} -3.45 \\ 0.32 \\ -0.34 \\ -0.31 \\ 0.30 \\ 0.29 \end{bmatrix}, b^2 = 0.45 \tag{11a}$$

For mixed convection:

$$w^1 = \begin{bmatrix} 2.96 & -0.92 & -0.84 \\ -0.55 & -1.07 & -1.64 \\ 0.81 & 0.75 & -0.75 \\ -0.07 & 0.11 & -0.04 \\ -0.84 & -0.82 & -0.55 \\ 0.25 & 0.44 & -0.48 \end{bmatrix},$$

$$w^2 = \begin{bmatrix} 3.21 & -2.01 & 0.50 & -0.30 & -1.44 & 0.12 \end{bmatrix},$$

$$b^1 = \begin{bmatrix} 2.30 \\ -0.73 \\ -1.02 \\ -1.20 \\ -0.36 \\ 0.04 \end{bmatrix}, b^2 = -0.17 \tag{11b}$$

As shown in Table 4, the total number of data points for forced convection is predicted within -12.2% to $+17.0\%$, and those for mixed convection are predicted within -11.1% to $+8.5\%$. More than 97% of all the data are predicted within $\pm 10\%$ deviation for the two convection modes. For forced convection, about 77% of all the data (164 data points) are predicted within $\pm 5\%$ deviation and the absolute mean deviation is about 3.6%. For the mixed convection, about 92% of all the data (308 data points) are predicted within $\pm 5\%$ deviation, and the absolute mean deviation is 2.4%. As compared to the results of the laminar heat transfer correlation given by Eq. (1) and presented in Table 1, significant improvement is observed.

For the calculation of the index of contribution for each variable, Eqs. (4–6) were employed according to the weight matrices, w^1 and w^2, given in Eqs. (11a) and (11b) for forced and mixed convection, respectively. The computation process is the same as that for the turbulent heat transfer data and is as follows:

1. For each hidden neuron k, the absolute value of the hidden-output layer connection weight is divided by the summation of the hidden-output layer connection weight, as seen in Eq. (4). The Q_k is computed for each neuron as follows:

Heat transfer mode	Hidden neuron 1	Hidden neuron 2	Hidden neuron 3	Hidden neuron 4	Hidden neuron 5	Hidden neuron 6
Forced convection	3.18	1.14	1.37	1.05	0.47	0.09
Mixed convection	3.21	2.01	0.50	0.30	1.44	0.12

Table 4 Prediction results for the improved laminar flow correlation developed based on the ANN method

Inlet configuration	Number of data within ±10%	Number of data within ±5%	Abs. mean dev. (%)	Abs. range of dev. (%)
Forced convection				
Total data points for all three inlets (212 pts.)	207	164	3.6	−12.2% to +17.0%
Re-entrant (84 pts.)	84	67	3.5	−8.9% to +9.6%
Square-edged (96 pts.)	91	67	4.0	−12.2% to +17.0%
Bell-mouth (32 pts.)	32	30	2.3	−5.3% to +6.1%
Mixed convection				
Total data points for dall three inlets (334 pts.)	333	308	2.4	−11.1% to +8.5%
Re-entrant (84 pts.)	83	81	2.3	−11.1% to +5.6%
Square-edged (198 pts.)	198	177	2.5	−6.5% to +8.5%
Bell-mouth (52 pts.)	52	50	1.9	−5.2% to +6.0%

See Eqs. (3) and (10) for the input vector (p) and Eq. (11) for the constant matrices and scalars (w^1, w^2, b^1, b^2).

2. For each hidden neuron k, multiply the Q_k by the absolute value of the hidden-input layer connection weight. Then, sum up the values to obtain the P_j for each input variable p_j, as seen in Eq. (5):

Heat transfer mode	Gz	Ra	μ_b/μ_w
Forced convection	2.25	0.38	1.53
Mixed convection	2.20	1.21	1.29

3. Compute the index of contribution in percentage by dividing P_j by the sum of the P_j corresponding to each input variable, as seen in Eq. (6). The index of contribution for each variable is:

Heat transfer mode	Gz	Ra	μ_b/μ_w
Forced convection	53.9%	9.2%	36.9%
Mixed convection	46.8%	25.7%	27.5%

From the above values of the index of contribution, it can be seen that for the forced convection data, Gz is the most important dimensionless parameter because the forced convection data is very near the entrance of the tube. On the other hand, Ra is the least important dimensionless parameter, because near the tube entrance, the secondary flow effect has not developed yet. For the mixed convection data, Gz is again the most important dimensionless parameter, because for laminar heat transfer, the thermal entry length is long. Compared to the forced convection data, Ra in this case is also important because the secondary flow effect has been established. For both forced and mixed convection cases, the viscosity ratio is important due to the significant effect of variation of physical properties. Therefore, it can be concluded that the index of contribution calculated based on the proposed method completely agrees with the physics of the problem.

A relative contribution analysis method similar to the one used in this study was also proposed by Garson [12]. The method was used in ecological modeling. The algorithm also interprets the connection weights for determination of the relative importance of each input variable of ANN. Gevrey et al. [13] provide a summary of the algorithm used by Garson [12] as represented below:

- For each hidden neuron k, multiply the absolute valve of the hidden-output layer connection weight by the absolute valve of the hidden-input layer connection weight. Repeat the process for each input variable j. The products P_{kj} are obtained.
- For each hidden neuron, divide P_{kj} by the sum for all the input variables to obtain Q_{kj}.
- For each input variable, sum the product S_j formed from the previous computations of Q_{kj}. Divide S_j by the sum for all the input variables. Expressed as a percentage, this gives the relative importance (RI) of all output weights attributed to the given input variables.

The Garson's algorithm also adopts the connection weights to compute the percent of relative importance of each input variable, but the algorithm is different from our proposed method. Therefore, it is worth comparing the method developed in this study with Garson's algorithm. Based on the same ANN 'weight' matrices for the turbulent and laminar heat transfer data, the comparison of the index of contribution obtained by the method of this study [index(p_j)] and the percent of relative importance computed by the Garson's algorithm (RI) is presented below.

For turbulent heat transfer data:

Contribution analysis method	Re	Pr	x/D	μ_b/μ_w
Present study	35.4%	42.4%	7.9%	14.3%
Garson [12]	30.1%	30.6%	19.5%	19.8%

For laminar heat transfer data:

Contribution analysis method	Gz	Ra	μ_b/μ_w
Present study			
Forced convection	53.9%	9.2%	36.9%
Mixed convection	46.8%	25.7%	27.5%
Garson [12]			
Forced convection	41.6%	21.9%	36.5%
Mixed convection	34.5%	35.0%	30.5%

According to the comparison of the results between the two methods, the Garson's algorithm can select Re and Pr to be the most important variables for the heat transfer in turbulent flow. This finding is in agreement with the index of contribution defined in this study. However, Garson predicted both of the ratios, x/D and μ_b/μ_w, to contribute nearly 20% each to the Nusselt number. The contribution of x/D by Garson's method is much higher than what the present method predicted (7.9%). Therefore, the Garson's algorithm cannot clearly identify x/D as the least important variable. For the forced convective laminar flow data, the relative importance of Ra predicted by Garson (21.9%) is much higher than the prediction of the present study (9.2%). Based on the physical phenomena, the importance of Ra should be less for the laminar forced convection. The Garson's algorithm method could not identify the low relative importance of Ra in laminar forced convection flow. For the mixed convection, it is obvious that Gz, Ra, and μ_b/μ_w, are all important. Therefore, both algorithms can reflect that. Overall, the performance of the method used in the present study is superior to the method of Garson in correctly identifying the most and least important variables in different cases.

SUMMARY AND CONCLUSIONS

In this study, the ANN method was applied to the laminar and turbulent heat transfer data of Ghajar and Tam [4], and appropriate heat transfer correlations were developed. An index of contribution was defined, and through contribution analysis, the relative importance of the associated independent variables was examined using the coefficient matrices of the ANN correlations. For the turbulent heat transfer data, the most important variables were the Reynolds and Prandtl numbers, and the least important variables turned out to be the length-to-diameter ratio and the bulk-to-wall viscosity ratio. The analysis was then extended to the more complicated laminar heat transfer data in the developing region. In this region, more parameters needed to be considered because the effects of entrance, buoyancy, and variation of properties are all important. The Graetz number, Rayleigh number, and bulk-to-wall viscosity ratio were selected as the key parameters. The analysis showed that the Graetz number is the most important variable in the laminar flow region and the Rayleigh number contributes significantly in the mixed convection region. The results of this study demonstrated that the proposed contribution analysis method correctly predicts the influence of different variables or a combination of them on complicated heat transfer problems.

The proposed method was also compared with a similar contribution analysis algorithm by Garson [12]. The results showed that the present method can represent the contribution of each variable more effectively than the method of Garson. The application of the proposed method to more complicated heat transfer problems to further verify its capability is recommended.

NOMENCLATURE

a	output vector
b	bias matrix
c_p	specific heat at constant pressure, kJ/(kg·K)
D	inside diameter of the tube, m
f	activation (or transfer) function
g	acceleration of gravity, m/s^2
Gr	local bulk Grashof number ($= g\beta\rho^2D^3(T_w\text{-}T_b)/\mu_b^2$)
Gz	local Graetz number ($=$ RePrD/x)
h	local peripheral heat transfer coefficient, W/(m^2·K)
h_b	local peripheral heat transfer coefficient at the bottom of tube, W/(m^2·K)
h_t	local peripheral heat transfer coefficient at the top of tube, W/(m^2·K)
k	thermal conductivity, W/(m^2·K)
Nu	local average or fully developed peripheral Nusselt number ($=$ hD/k)
Nu_l	local average or fully developed peripheral laminar Nusselt number
Nu_t	local average or fully developed peripheral turbulent Nusselt number
p	input vector
P_j	contribution of the jth independent variable p_j
Pr	local bulk Prandtl number ($= c_p\mu_b$ /k)
Q_k	contribution of the kth neuron output to the ANN model
Ra	local bulk Rayleigh number ($=$ GrPr)
Re	local bulk Reynolds number ($= \rho VD/\mu_b$)
T_b	local bulk temperature, °C
T_w	local wall temperature, °C
V	average velocity in the test section, m/s
W	weight matrix
x	local distance along the test section from the inlet, m

Greek Symbols

β	local bulk coefficient of thermal expansion, K^{-1}
μ_b	local bulk dynamic viscosity, Pa·s
μ_w	local wall dynamic viscosity, Pa·s

ρ local bulk density, kg/m^3

Subscripts

i	dummy parameter
j	jth input variable
k	kth hidden neuron
max	maximum value
min	minimum value
R	number of inputs
S	number of hidden neurons

Superscripts

1	the hidden layer of the ANN model
2	the output layer of the ANN model

REFERENCES

[1] Kakac, S., Shah, R. K., and Aung, W., *Handbook of Single-Phase Convective Heat Transfer*, Wiley, New York, 1987.

[2] Tam, L. M., and Ghajar, A. J., Transitional Heat Transfer in Plain Horizontal Tubes, *Heat Transfer Engineering*, vol. 27, no. 5, pp. 23–38, 2006.

[3] Ghajar, A. J., Tam, L. M., and Tam, S. C., Improved Heat Transfer Correlation in the Transition Region for a Circular Tube with Three Inlet Configurations Using Artificial Neural Networks, *Heat Transfer Engineering*, vol. 25, no. 2, pp. 30–40, 2004.

[4] Ghajar, A. J., and Tam, L. M., Heat Transfer Measurements and Correlations in the Transition Region for a Circular Tube with Three Different Inlet Configurations, *Experimental Thermal and Fluid Science*, vol. 8, no. 1, pp. 79–90, 1994.

[5] Ghajar, A. J., and Kim, J., Calculation of Local Inside-Wall Convective Heat Transfer Parameters from Measurements of the Local Outside-Wall Temperatures along an Electrically Heated Circular Tube, in *Heat Transfer Calculations,* ed. Myer Kutz, pp. 23.3–23.27, McGraw-Hill, New York, 2006.

[6] Ghajar, A. J., and Tam, L. M., Flow Regime Map for a Horizontal Pipe with Uniform Heat Flux and Three Different Inlet Configurations, *Experimental Thermal and Fluid Science*, vol. 10, no. 3, pp. 287–297, 1995.

[7] Martinelli, R. C., and Boelter, L. M. K., The Analytical Prediction of Superposed Free and Forced Viscous Convection in a Vertical Pipe, *Univ. Calif. Publ. Eng.,* vol. 5, no. 2, p. 23, 1942.

[8] Sieder, E. N., and Tate, G. E., Heat Transfer and Pressure Drop in Liquids in Tubes, *Ind. Eng. Chem.*, vol. 28, pp. 1429–1435, 1936.

[9] Hornik, K., Approximation Capabilities of Multilayer Feedforward Networks, *Neural Networks*, vol. 4, no. 2, pp. 251–257, 1991.

[10] Rumelhart, D. E., Hinton, G. E., and Williams, R. J., Learning Internal Representations by Error Propagation, in *Parallel Distributed Processing: Explorations in the Microstructure of Cognition,* eds. D. E. Rumelhart and J. L. McClelland, vol. 1, pp. 318–362, MIT Press, Cambridge, Mass., 1986.

[11] Hagan, M. T., and Menhaj, M. B., Training Feedforward Networks with Marquardt Algorithm, *IEEE Transactions on Neural Networks*, vol. 5, no. 6, pp. 989–993, 1994.

[12] Garson, G. D., Interpreting Neural Network Connection Weights, *Artificial Intelligence Expert*, vol. 6, pp. 47–51, 1991.

[13] Gevrey, M., Dimopoulos, I., and Lek, S., Review and Comparison of Methods to Study the Contribution of Variables in Artificial Neural Network Models, *Ecological Modeling*, vol. 160, pp. 249–264, 2003.

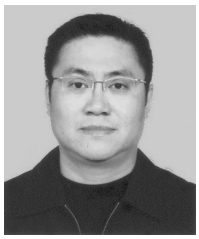

Lap Mou Tam received his Ph.D. in 1995 from Oklahoma State University, School of Mechanical and Aerospace Engineering, Stillwater, Oklahoma. In 1996, he joined the University of Macau as an assistant professor and is now a professor and department head of electromechanical engineering at the University of Macau, Macau, China. In 2001, he was appointed by the University of Macau to serve as the chairman of board of directors in the Institute for the Development and Quality, a non-profit institute providing mechanical- and electromechanical-related engineering services to the public. His research interests include single- and multi-phase heat transfer, chaos, fire engineering, and indoor air quality. He is a senior member of the Chinese Mechanical Engineering Society.

Afshin J. Ghajar is a regents professor and director of Graduate Studies in the School of Mechanical and Aerospace Engineering at Oklahoma State University. He received his B.S., M.S., and Ph.D., all in mechanical engineering from Oklahoma State University. His expertise is in experimental and computational heat transfer and fluid mechanics. Dr. Ghajar has been a summer research fellow at Wright Patterson AFB (Dayton, Ohio) and Dow Chemical Company (Freeport, Texas). He and his coworkers have published more than 130 reviewed research papers. He has received several outstanding teaching/service awards, such as the Regents Distinguished Teaching Award, Halliburton Excellent Teaching Award; Mechanical Engineering Outstanding Faculty Award for Excellence in Teaching and Research; Golden Torch Faculty Award for Outstanding Scholarship, Leadership, and Service by the Oklahoma State University/National Mortar Board Honor Society; and the College of Engineering Outstanding Advisor Award for commitment to students as demonstrated by exceptional advising and outstanding student success. Dr. Ghajar is a fellow of the American Society of Mechanical Engineers (ASME), and Editor-in-Chief of *Heat Transfer Engineering*.

Hou Kuan Tam is currently a Ph.D. candidate at the University of Macau, Department of Electromechanical Engineering, Macau, China. His research interests are the artificial neural networks, single- and multiphase heat transfer, and the application of computation intelligence.